

## Relaxation of Ni(111) Surface by Oxygen Adsorption

T. Narusawa and W. M. Gibson

*Department of Physics, State University of New York at Albany, Albany, New York 12222*

and

E. Törnqvist

*Department of Physics and Laboratory for Research on the Structure of Matter, University of Pennsylvania, Philadelphia, Pennsylvania 19104*

(Received 11 May 1981)

We have shown by displacement-sensitive high-energy He<sup>+</sup>-ion scattering that the clean Ni (111) surface has a bulklike structure with ~20% enhancement of surface thermal vibration, and that the  $p(2 \times 2)$  and  $(\sqrt{3} \times \sqrt{3})R30^\circ$  superstructures on the oxygen-adsorbed surface are accompanied by expansion of the first nickel layer by ~0.15 Å. In addition, the absolute oxygen coverages for these two superstructures and at saturation were measured to be  $\sim \frac{1}{4}$ ,  $\sim \frac{1}{3}$ , and ~3 monolayers, respectively.

PACS numbers: 68.20.+t, 61.80.Mk, 79.20.Ne

Adsorption-induced superstructures have long been a subject for low-energy electron-diffraction (LEED) studies. The superstructures can arise if the adsorbates are ordered and/or the substrate reconstructs in the appropriate symmetry. Since these two possibilities give apparently the same LEED pattern, it is often difficult to discriminate by LEED measurements alone. In the particular case of oxygen on (110) and (111) nickel, Demuth and Rhodin<sup>1</sup> suggested from their LEED measurements that oxygen adsorption at room temperature induces negligible substrate disruption. Marcus, Demuth, and Jepsen<sup>2</sup> carried out dynamical LEED calculations assuming ordered layers on the bulklike lattice and obtained the O-Ni bonding length and preferred adsorption sites. However, an ion scattering study of the oxygen-Ni(110) system by Smeenk *et al.*<sup>3</sup> has clearly shown that the substrate surface lattice is distorted from the very initial stage of adsorption, though they have not mentioned it explicitly.

The present MeV-ion scattering study shows clear stages of relaxation of the (111) nickel surface lattice which is correlated with the  $p(2 \times 2)$  and  $(\sqrt{3} \times \sqrt{3})R30^\circ$  oxygen-adsorption superstructures. The relaxation is about 0.15 Å outward and perpendicular to the surface. These superstructures are associated with only minor changes in the LEED integral-order beam intensity spectra compared with the clean surface. Consequently the substrate relaxation was undetected from the LEED analysis. In addition, the ion scattering measurements allow absolute oxygen coverage determinations that confirm  $\sim \frac{1}{4}$  of a monolayer coverage for the  $p(2 \times 2)$  structure,  $\sim \frac{1}{3}$  of a monolayer for the  $(\sqrt{3} \times \sqrt{3})R30^\circ$  structure, and ~3 monolayers at saturation. It is also shown that

at room temperature, saturation with oxygen results in the incorporation of ~3 monolayers of nickel in an amorphous oxide film having a NiO stoichiometry and that reconstruction of relaxation in the underlying nickel single crystal is less than 0.05 Å. Our data also provide a natural explanation of certain unexplained features in the oxygen-Ni(111) temperature versus coverage phase diagram.

Clean Ni(111) surfaces were prepared in UHV by oxidation-reduction cycles and by Ar<sup>+</sup>-ion sputtering and annealing. The cleanliness and symmetry of the crystal surface were examined by Auger electron spectroscopy (AES) and medium-energy electron diffraction. In accordance with previous studies,<sup>1, 4</sup> we found two well-defined superstructures,  $p(2 \times 2)$  and  $(\sqrt{3} \times \sqrt{3})R30^\circ$ , in the course of oxygen adsorption on the clean surface at room temperature. *In situ* high-energy (~0.5–2.0 MeV) He<sup>+</sup>-ion scattering measurements were carried out in both normal and off-normal axial channeling directions. The main signal quantity measured in our experiment is the surface peak (SP) intensity which is sensitive and directly related to the substrate surface atomic structure and dynamics. The sensitivity increases with the incident energy of the projectile and is limited to displacements of the surface atoms in a direction perpendicular to the incident beam direction. Experimental results are compared with computer calculations of the nuclear encounter probability in which the paths of charged particles were traced in a stepwise manner by using the binary collision approximation. Details about the computer simulations<sup>5</sup> and the nature and measurements<sup>6</sup> of the SP intensity have been discussed elsewhere.

Figure 1 shows the energy dependence of SP intensity from the clean surface aligned in the  $\langle 110 \rangle$  off-normal direction. The units of SP intensity, atoms/row, express how many atoms in an atomic string along the incident direction contribute to the SP intensity. The monotonic increase of the SP intensity with the incident energy corresponds to a decrease of the shadowing of underlying atoms by the surface atoms. Computer simulations were carried out for a number of models of the surface atomic structure and dynamics. Two of them are shown in Fig. 1: Curve *a* assumes a bulklike structure and a bulklike thermal vibration; curve *b* assumes a bulklike structure with a small enhancement in the surface thermal vibration. A good agreement between the plotted experimental data and curve *b* together with the  $(1 \times 1)$  diffraction pattern strongly suggests that the clean Ni(111) surface is actually bulklike. Detailed angular distribution scans through the  $\langle 110 \rangle$  direction confirmed this conclusion since they showed a symmetric and unshifted profile relative to the bulk crystal angular distribution. The result is therefore clear that a clean Ni(111) surface is bulklike with a relaxation or recon-

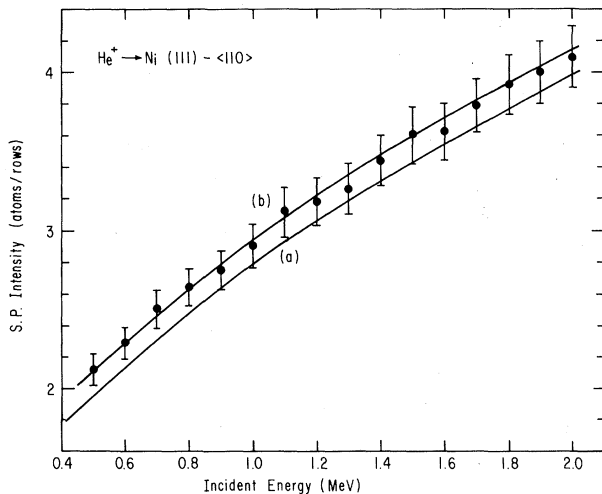


FIG. 1. Energy dependence of  $\langle 110 \rangle$  surface peak intensity for a clean Ni (111) surface. Simulation curve *a* assumes a bulklike structure and isotropic bulklike thermal vibration, i.e., one-dimensional rms amplitude of  $0.068 \text{ \AA}$  which is calculated with use of the bulk Debye temperature of 420 K and the target temperature of 310 K during the measurements. Simulation curve *b* assumes a bulklike structure and an enhanced surface thermal vibration, i.e., one-dimensional rms amplitudes of  $0.084 \text{ \AA}$  for the first layer,  $0.077 \text{ \AA}$  for the second layer,  $0.072 \text{ \AA}$  for the third layer, and  $0.068 \text{ \AA}$  for the fourth and underlying layers.

struction no greater than  $0.02 \text{ \AA}$  and with a modest enhancement ( $\sim 20\%$ ) in thermal vibration amplitude of the first atomic layers.

When the clean (111) nickel surface is exposed to oxygen gas, the  $(1 \times 1)$  diffraction pattern gradually changes to a  $p(2 \times 2)$  and then to a  $(\sqrt{3} \times \sqrt{3})R30^\circ$  pattern eventually smearing out at an exposure of about 10 L ( $1 \text{ L} = 1 \times 10^{-6} \text{ Torr sec}$ ). The exposures which apparently lead to the most intense patterns are  $\sim 2$  and  $\sim 5 \text{ L}$  for each superstructure, respectively. The fractional oxygen coverage at each of these stages was measured by AES calibrated by MeV-He<sup>+</sup>-ion scattering. Assuming linearity between the O *KLL* Auger peak intensity and the coverage in the submonolayer range, we can conclude that the oxygen coverage is  $0.23 \pm 0.04$  monolayers for the  $p(2 \times 2)$  structure and  $0.31 \pm 0.05$  monolayers for the  $(\sqrt{3} \times \sqrt{3})R30^\circ$  structure. Corresponding to the development of superstructures the SP intensity of Ni at 2 MeV behaves as shown in Fig. 2. Most strikingly, the  $\langle 110 \rangle$  SP intensity shows clear stages of increase, whereas the  $\langle 111 \rangle$  SP intensity shows no increase up to an exposure of  $\sim 10 \text{ L}$ . The only explanation of this difference is that the nickel surface atoms

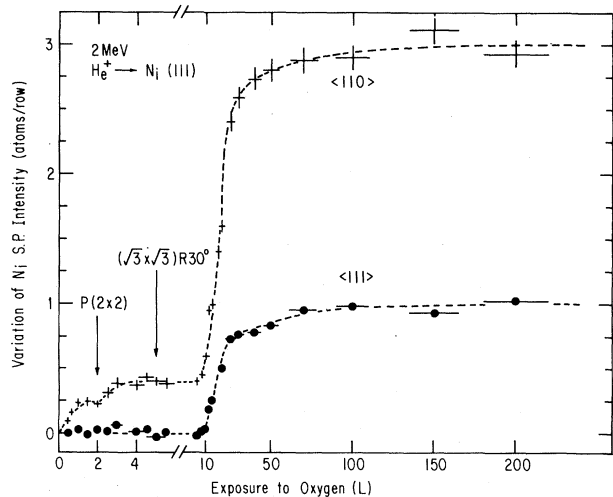


FIG. 2. Variation of  $\langle 111 \rangle$  and  $\langle 110 \rangle$  nickel surface peak intensities at 2 MeV as a function of exposure to oxygen ( $1 \text{ L} = 1 \times 10^{-6} \text{ Torr sec}$ ). Exposures which give the most intense superstructure diffraction patterns are indicated by arrows. Since the incident beam sees the top three layers directly in the  $\langle 111 \rangle$  direction, an increase of the  $\langle 111 \rangle$  SP intensity by 1 atom/row corresponds to displacements of three nickel layers if the displacements are large enough ( $\geq 0.3 \text{ \AA}$ ) and do not correlate with each other. Similarly the increase of the  $\langle 110 \rangle$  SP intensity by 1 atom/row corresponds to displacements of one monolayer.

relax in a direction perpendicular to the surface as a result of the submonolayer oxygen adsorption. Since the increase of the SP intensity depends on both the magnitude of the displacements and the number of the displaced atoms, Fig. 2 alone cannot lead us to a unique structure model. For example, the increase of the SP intensity by  $\sim 0.4$  atoms/row at the  $(\sqrt{3}\times\sqrt{3})R30^\circ$  stage is consistent with both of the following models, one which assumes a uniform relaxation of the entire first nickel layer by  $\sim 0.15$  Å and another which assumes a large relaxation ( $\approx 0.3$  Å) of  $\sim \frac{1}{3}$  of the first nickel layer only. To differentiate between these choices we measured angular distributions of the nickel SP intensities for the  $\langle 110 \rangle$  axial direction and compared them with computer simulations.

In contrast to the clean surface case, the  $p(2\times 2)$  and  $(\sqrt{3}\times\sqrt{3})R30^\circ$  superstructures show significant asymmetry about the  $\langle 110 \rangle$  direction as shown in Fig. 3 for the  $(\sqrt{3}\times\sqrt{3})R30^\circ$  case. The solid curve in Fig. 3 is the best-fit result of simulation and suggests that the first nickel layer is uniformly relaxed outward (lattice expansion) by 0.15 Å. This is clearly superior to a model in which one-third of the nickel atoms are re-

laxed by a large amount as suggested above and as shown by the broken curve in Fig. 3. It must be noted that some ambiguity about the uniqueness of this structure model remains since we cannot rule out a complicated case, such as that the majority of the first-layer atoms, say  $\frac{2}{3}$  monolayers, relaxed by 0.18 Å and the remainder relaxed by 0.12 Å. However, since there is no model based on either LEED or low- and high-energy ion scattering data to suggest such a complicated structure, we feel that the evidence is strong to support the simple structure indicated by the solid curve in Fig. 3, i.e., that all atoms in the first layer are relaxed outward by  $0.15 \pm 0.02$  Å. Similar experimental plots for the  $p(2\times 2)$  structure are fitted most closely by a structure model in which  $\frac{3}{4}$  monolayers are expanded by 0.15 Å and  $\frac{1}{4}$  monolayers are expanded a little or not at all. However, one cannot eliminate the possibility of uniform expansion of the entire monolayer by  $\sim 0.12$  Å. It is interesting to note that the former combination model is closely correlated to the threefold symmetry sites proposed as the preferred adsorption sites for oxygen on the (111) nickel surface. In any case there is no doubt about an outward relaxation of the first nickel layer due to the submonolayer oxygen adsorption. Recently Roelofs *et al.*<sup>7</sup> have reported results on the  $T$  vs  $\theta$  (temperature versus coverage) phase diagram of oxygen on Ni(111). They have tried to model this phase diagram theoretically by a set of oxygen-oxygen and oxygen-substrate interaction parameters. Their success was somewhat limited and it was suggested that a substrate reconstruction might be the cause of this. Our data justify that assumption.

The increase of the SP intensity in both incident directions at an exposure of about 10 L corresponds to the onset of displacements of the nickel atoms in both the lateral and the longitudinal directions. This is an indication of penetration of the oxygen atoms into subsurface sites at these stages which converts an ordered surface structure to a disordered one. The apparent saturation of the SP intensity in both the  $\langle 111 \rangle$  and  $\langle 110 \rangle$  cases indicate that  $\sim 3$  monolayers of nickel are released from the lattice frame. This, together with the ion scattering measurements of oxygen coverage of  $2.8 \pm 0.4$  monolayers at saturation, indicates formation of an amorphous oxide film having a NiO stoichiometry. It was also shown by measurements of the energy and angular dependence of the nickel SP intensity that nickel lattice atoms at the interface between the amor-

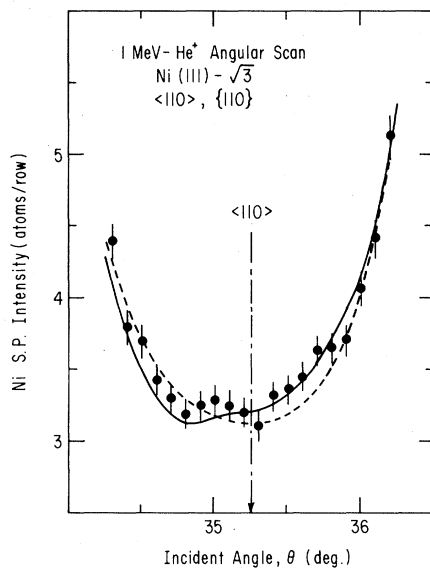


FIG. 3. Angular dependence of  $\langle 110 \rangle$  surface peak intensity at 1 MeV from the  $(\sqrt{3}\times\sqrt{3})R30^\circ$  oxygen-adsorbed Ni (111) surface. The incident beams scans in the  $\{110\}$  plane. The solid curve is the result of a computer simulation which assumes a uniform outward relaxation of the first nickel layer by 0.15 Å. The broken line assumes that  $\frac{1}{3}$  of the surface Ni atoms are relaxed by 0.30 Å and  $\frac{2}{3}$  are not relaxed.

phous oxide film and the nickel single crystal are not displaced within the accuracy of the measurements ( $0.05 \text{ \AA}$ ), i.e., the interface is very sharp and unstrained. These results about oxide formation agree quite well with the conclusions of previous studies except for the oxide film thickness at saturation.<sup>3,8,9</sup>

In conclusion we have measured the SP intensity in the  $\langle 111 \rangle$  and  $\langle 110 \rangle$  directions in the course of oxygen adsorption and oxidation of the Ni(111) surface at room temperature. The energy and angular dependence of the SP intensity showed that the clean Ni(111) surface has a bulklike structure with  $\sim 20\%$  enhancement of the surface thermal vibration. The dynamics of the surface do not change appreciably as a result of the oxygen adsorption. The angular dependence of the  $\langle 110 \rangle$  SP intensity indicated that the  $p(2 \times 2)$  and  $(\sqrt{3} \times \sqrt{3})R30^\circ$  superstructures are associated with outward relaxation of the first nickel layer by  $\sim 0.15 \text{ \AA}$ . This magnitude of the relaxation depends on the validity of the computer simulations; however, our experimental data provide the first definitive and direct evidence of relaxation in the oxygen-induced superstructures of the Ni(111) surface. The absolute oxygen coverage measured by ion scattering and AES is  $\sim \frac{1}{4}$  and  $\sim \frac{1}{3}$  monolayers for the  $p(2 \times 2)$  and  $(\sqrt{3} \times \sqrt{3})R30^\circ$  structures, respectively. These models are best fitted with a model in which the oxygen adsorbs on the three-fold sites and the (three) nearest neighbors of the adsorbate atoms relax outwards. A consequence of this model is that the  $p(2 \times 2)$  pattern observed by LEED is not just a signature of the order of the adlayer but is also caused by the periodicity of the substrate surface. Also shown were the

formation of an amorphous NiO film which incorporates  $\sim 3$  monolayers of Ni at saturation and a very sharp interface between the oxide film and the underlying crystal. Details of the measurements including effects of heating the substrate crystal will be published separately.<sup>10</sup>

Acknowledgment is due to L. C. Feldman, Bell Laboratories, and T. Gustafsson and E. W. Plummer, University of Pennsylvania, for helpful suggestions and stimulating discussions. This work was supported by the U. S. Office of Naval Research under Contracts No. N00014-78-C-0616 and No. N00014-79-C-0991.

<sup>1</sup>J. E. Demuth and T. N. Rhodin, *Surf. Sci.* **45**, 249 (1974).

<sup>2</sup>P. M. Marcus, J. E. Demuth, and D. W. Jepsen, *Surf. Sci.* **53**, 501 (1975).

<sup>3</sup>R. G. Smeenk, R. M. Tromp, J. F. Van der Veen, and F. W. Saris, *Surf. Sci.* **95**, 156 (1980).

<sup>4</sup>L. D. Roelofs, T. L. Einstein, P. E. Hunter, A. R. Kortan, R. L. Park, and R. M. Roberts, *J. Vac. Sci. Technol.* **17**, 231 (1980).

<sup>5</sup>J. H. Barrett, *Phys. Rev. B* **3**, 1527 (1971); S. T. Picraux, W. L. Brown, and W. M. Gibson, *Phys. Rev. B* **6**, 1382 (1972); I. Stensgaard, L. C. Feldman, and P. J. Silverman, *Surf. Sci.* **77**, 513 (1978).

<sup>6</sup>L. C. Feldman, P. J. Silverman, and I. Stensgaard, *Surf. Sci.* **87**, 410 (1979); L. C. Feldman, in *Surface Science: Recent Progress and Perspectives*, edited by R. Vanselow (CRC Press, Cleveland, Ohio, 1980).

<sup>7</sup>L. D. Roelofs, A. R. Kortan, T. L. Einstein, and R. L. Park, *J. Vac. Sci. Technol.* **18**, 492 (1981).

<sup>8</sup>P. H. Holloway and J. B. Hudson, *Surf. Sci.* **43**, 123 (1974).

<sup>9</sup>P. H. Holloway, *J. Vac. Sci. Technol.* **18**, 653 (1981).

<sup>10</sup>T. Narusawa, W. M. Gibson, and E. Törnqvist, to be published.